AD-A054 107 POLYTECHNIC INST OF NEW YORK FARMINGDALE F/G 20/14
GROUND WAVE PROPAGATION IN THE PRESENCE OF SMOOTH HILLS AND DEP--ETC(U)
1975 L B FELSEN, A GREEN DAHC04-75-G-0152
UNCLASSIFIED ARO-13126.2-EL NL

END
DATE FILMED
6-78
DDC

(2)



# AGARD

ADVISORY GROUP FOR AEROSPACE RESEARCH & DEVELOPMENT

7 RUE ANCELLE 92200 NEUILLY SUR SEINE FRANCE

Paper Reprinted from - Ao44F00
Conference Proceedings No.208 - dated June 77

## EM Propagation Characteristics of Surface Materials and Interface Aspects



NORTH ATLANTIC TREATY ORGANIZATION

Unclassified

SECURITY CLASSIFICATION OF THIS PAGE (When Data Entered)

| REPORT DOCUMENTATION PAGE | READ INSTRUCTIONS BEFORE COMPLETING FORM |
|---|---|
| 1. REPORT NUMBER: 13126.2-EL (28 ARO) | 2. GOVT ACCESSION NO. / 3. RECIPIENT'S CATALOG NUMBER |
| 4. TITLE (and Subtitle): GROUND WAVE PROPAGATION IN THE PRESENCE OF SMOOTH HILLS AND DEPRESSIONS, | 5. TYPE OF REPORT & PERIOD COVERED: Reprint |
| | 6. PERFORMING ORG. REPORT NUMBER |
| 7. AUTHOR(s): L. B. Felsen, A. Green | 8. CONTRACT OR GRANT NUMBER(s): DAHC04-75-G-0152 |
| 9. PERFORMING ORGANIZATION NAME AND ADDRESS: Polytechnic Institute of NY, Farmington, NY 11735 | 10. PROGRAM ELEMENT, PROJECT, TASK AREA & WORK UNIT NUMBERS |
| 11. CONTROLLING OFFICE NAME AND ADDRESS: U. S. Army Research Office, P. O. Box 12211, Research Triangle Park, NC 27709 | 12. REPORT DATE: 1975 / 13. NUMBER OF PAGES: 13 (12 15p.) |
| 14. MONITORING AGENCY NAME & ADDRESS (if different from Controlling Office) | 15. SECURITY CLASS. (of this report): unclassified / 15a. DECLASSIFICATION/DOWNGRADING SCHEDULE |

16. DISTRIBUTION STATEMENT (of this Report)

Approved for public release; distribution unlimited.

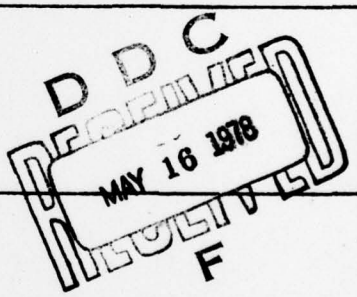


17. DISTRIBUTION STATEMENT (of the abstract entered in Block 20, if different from Report)

18. SUPPLEMENTARY NOTES

The findings in this report are not to be construed as an official Department of the Army position, unless so designated by other authorized documents.

19. KEY WORDS (Continue on reverse side if necessary and identify by block number)

20. ABSTRACT (Continue on reverse side if necessary and identify by block number)

Electromagnetic waves propagating along the ground-air interface are influenced markedly by terrain features. Previous studies have dealt extensively with abrupt changes in surface properties (modeled in terms of surface impedance), or abrupt changes in height as represented by precipitous hills or valleys, on the convexly curved earth's surface. the terrain changes gradually, as in the presence of smooth hills or depressions, it is necessary to consider the effects of variable concave surface curvature, and more generally those of a gradual changeover from concave to convex, on the signal propagation characteristics. Of special interest are the fields observed on or near the surface when the source is also situated on or near the surface. This paper is concerned with a review of earlier work on the concave surface problem, and with a summary of our current effort to adapt and extend these results to ground wave propagation.

DD FORM 1 JAN 73 1473 EDITION OF 1 NOV 65 IS OBSOLETE

Unclassified

SECURITY CLASSIFICATION OF THIS PAGE (When Data Entered)

AD B 792

# GROUND WAVE PROPAGATION IN THE PRESENCE OF SMOOTH HILLS AND DEPRESSIONS*

L. B. Felsen and A. Green
POLYTECHNIC INSTITUTE OF NEW YORK
Farmingdale, N. Y. 11735 USA

## I. INTRODUCTION

Electromagnetic waves propagating along the ground-air interface are influenced markedly by terrain features. Previous studies have dealt extensively with abrupt changes in surface properties (modeled in terms of surface impedance), or abrupt changes in height as represented by precipitous hills or valleys, on the convexly curved earth's surface. When the terrain changes gradually, as in the presence of smooth hills or depressions, (Fig. 1), it is necessary to consider the effects of variable concave surface curvature, and more generally those of a gradual changeover from concave to convex, on the signal propagation characteristics. Of special interest are the fields observed on or near the surface when the source is also situated on or near the surface. This paper is concerned with a review of earlier work on the concave surface problem, and with a summary of our current effort to adapt and extend these results to ground wave propagation.

The most fundamental difference between the excitation of concave and convex surfaces of large (compared to the wavelength) radius of curvature is the absence in the former of a geometrical shadow region, from which the source is invisible. This circumstance gives rise not only to a more intricate geometric-optical field comprising multiply reflected rays (Fig. 2) but also, in an alternative guided wave description, to the presence of whispering gallery modes which cling to the surface (Fig. 3) and, in the absence of dissipation, experience no attenuation. Their counterparts on a convex surface, the creeping waves, lose energy by tangential shedding along the propagation path. The problem is complicated further by the fact that ray optics is incapable of providing the field solution since the caustics of multiply reflected rays pile up near the boundary (Fig. 2) and thus invalidate the geometric-optical field evaluation there. A field representation in terms of whispering gallery modes only (with inclusion of a continuous mode spectrum for some surfaces), while valid, is inconvenient for calculation for large separation of source and observation points on a large-radius surface since the number of modes required can be substantial. These problems do not arise on a convex surface where the distant field in the shadow region is represented compactly by the dominant creeping wave.

To gain a better physical as well as quantitative understanding of these aspects of wave propagation on a concave surface, intensive studies have been carried out on the simplest prototype configuration, the interior of a perfectly reflecting circular cylinder (KINBER, B. YE, 1961; BABICH, V. M. and BULDYREV, V. S., 1972; WASYLKIWSKYJ, W., 1975). These two-dimensional field calculations, corresponding to excitation by an axial line source, are reviewed in Section II. A peculiarity of the cylindrical geometry is the presence, in addition to the whispering gallery modes, of a continuous guided mode spectrum which arises because of spurious reflections from the radial coordinate origin. Elimination of these spurious contributions leads to an asymptotic field representation in terms of an integral which can be manipulated so as to exhibit ray-optical contributions, whispering gallery mode contributions, a mixture of these, or a formulation containing a reduced canonical integral analogous to the Fock integral for convex surfaces. The most effective choice depends on the parameters of the problem. The results so obtained can be generalized to apply to arbitrary concave surface shapes provided that the radius of curvature changes slowly over a wavelength interval. The validity of these variable-curvature solutions has been verified by comparison with exact calculations performed for a parabolic contour (BULDYREV, V. M. and LANIN, A. I., 1975). These earlier investigations are reviewed, relevant numerical results presented and their physical implications discussed.

We have extended the analysis to track the field behavior when the radius of curvature of a circular cylindrical surface between fixed source and observation points changes from concave to convex; this transition from a curved to a flat boundary and beyond was not included in the earlier studies. We have also introudced the generalization for a lossy ground modeled by a surface impedance boundary condition (Section III).

The two-dimensional results are useful for the investigation of fields with broad phase fronts that do not vary appreciably along the axial direction of an elongated depression (gulley) or smooth ridge. When the incident phase front is strongly curved, as is the case when a dipole radiator is located within or near the ground perturbation, it is necessary to calculate the three-dimensional fields. These modifications are under study.

Still to be explored is the field description along surface contours that vary smoothly from concave to convex. This important problem is presently being investigated, as is the extension of the analysis to three-dimensional ground perturbations exemplified by spherical depressions.

---

* This work was performed under Contract No. DAHC 04-75-G=0152, U. S. Army Research Office - Durham, N. C.

## II. PERFECTLY CONDUCTING CIRCULAR BOUNDARY (TWO-DIMENSIONAL)

### A. Green's Function Formulation

We summarize here the results obtained in the literature on the prototype problem of line source radiation inside a perfectly conducting circular cylinder of radius a. To make the analysis relevant to the propagation along concave surfaces in general, it is necessary to remove the azimuthal periodicity imposed on the fields in the cylindrical $\underline{\rho} = (\rho, \phi)$ geometry, where $\rho$ represents the radial and $\phi$ the angular (azimuthal) coordinate. This can be done by extending the range of the $\phi$ coordinate from its physical periodic domain $0 \leq \phi \leq 2\pi$ into an infinite domain $-\infty < \phi < \infty$ (FELSEN, L. B. and MARCUVITZ, N., 1973). Such an extension implies that angularly propagating waves originating at the source point $(\rho', \phi')$ are outgoing toward $|\phi| = \infty$; this "angular radiation condition" can be realized by placing at some angular location away from the source angle $\phi'$ a perfect absorber for angularly propagating waves. Such an absorber has, however, the undesired property of generating diffraction at the radial coordinate origin $\rho = 0$. Therefore, when considering propagation phenomena ascribable only to the cylinder surface, it is desirable to remove the spurious diffraction effects from the total field solution.

The line source Green's function $G(\underline{\rho}, \underline{\rho}')$ in the cylindrical domain $0 < \rho < a$, $-\infty < \phi < \infty$, can be constructed by the method of separation of variables and expressed in its most general form as a contour integral involving the two one-dimensional characteristic Green's functions $g_\rho$ and $g_\phi$ for the radial and angular domains, respectively (FELSEN, L. B. and MARCUVITZ, N., 1973). As noted in Section I, when the Green's function is represented in terms of angularly propagating waves, the corresponding eigenmode spectrum in the radial domain involves a discrete (whispering gallery mode) and continuous portion. The latter accounts in part for propagation phenomena associated with the portion of the concave boundary lying between the source and observation points (this is desired contribution), and in part for the spurious diffraction effects of the angular absorber. When the spurious effects are removed and cognizance is taken of the high-frequency nature of the analysis, one may show that the relevant propagation characteristics along the portion of the concave boundary lying between the source point Q and the observation point P in Fig. 2 are contained in the partial Green's function (BABICH, V. M. and BULDYREV, F. S., 1972)

$$G_o(\underline{\rho}, \underline{\rho}') = \frac{1}{i(\pi ka)^2} \int_C \frac{e^{i\nu|\phi - \phi'|}}{H_\nu'^{(2)}(ka)\, J_\nu'(ka)}\, d\nu \tag{1}$$

where k is the free-space wavenumber, the prime on the cylinder functions denotes the derivative with respect to the argument, and a time factor $\exp(-i\omega t)$ is implied. It has been assumed in (1) that P and Q both lie on the boundary (i.e., $\rho = \rho' = a$) and that the boundary condition requires that the normal derivative of the Green's function vanishes at $\rho = a$; this makes $G_o$ proportional to the axial component of magnetic field. The contour C and the singularities of the integrand in the complex $\nu$-plane are shown in Figure 4. Contributions from the pole singularities $\nu_m$ arising from

$$J_{\nu_m}'(ka) = 0 \quad , \quad m = 1, 2, \ldots \tag{2}$$

are found to describe whispering gallery modes. While (2) has an infinite number of real solutions as indicated in Fig. 4, only those with $\mathrm{Re}\ \nu_m > 0$ represent spectral contributions in the angular transmission representation which includes also a continuous spectrum.

### B. Ray-optical Representation

The integralin (1) may be dealt with in various ways which exhibit the role of whispering gallery modes, ray-optical fields, or a combination of these, as noted in Section I. If an evaluation is sought by the method of steepest descent, one replaces $H_\nu'^{(2)}$ and $J_\nu' = (H_\nu'^{(1)} + H_\nu'^{(2)})/2$ by their Debye asymptotic forms

$$H_\nu'^{(1,2)}(ka) \sim \sqrt{\frac{2\cos w}{\pi ka}}\, \exp\left\{\mp ika\left[\cos w - (\tfrac{\pi}{2} - w)\sin w\right] \mp i\tfrac{\pi}{4}\right\} \tag{3}$$

$$\mathrm{Re}\ w > 0, \quad \left\{ka\left[\cos w - (\tfrac{\pi}{2} - w)\sin w\right]\right\}^{2/3} >> 1 \tag{3a}$$

where $\nu = ka \sin w$. Utilizing the traveling wave expansion

$$\frac{1}{J_\nu'(ka)} = \frac{2}{H_\nu'^{(2)}(ka)} \sum_{n=0}^{\infty} (-1)^n r^n, \quad r = \frac{H_\nu'^{(1)}(ka)}{H_\nu'^{(2)}(ka)} \quad , \quad |r| < 1 \quad , \tag{4}$$

in conjunction with (3), one reduces (1) to a series of integrals

$$G_o \sim \frac{1}{\pi} \sum_{n=0}^{\infty} (-i)^n \int_{C_n} \exp [ika\, q_n(w)]\, dw \tag{5}$$

where

$$q_n(w) = |\phi - \phi'| \sin w + 2(n+1) \left[\cos w - (\tfrac{\pi}{2} - w) \sin w\right] \quad . \tag{6}$$

The saddle points of $q_n(w)$, as obtained from $dq_n/dw = 0$, are

$$w_{sn} = \frac{\pi}{2} - \frac{|\phi - \phi'|}{2(n+1)} \quad , \quad \overline{w}_s = \frac{\pi}{2} \quad , \tag{7}$$

and thus lie on the real w axis between $w = 0$ and $w = \pi/2$. A typical path $C_n$ through the nth saddle point is shown in Figure 5. The original path mapped from the $\nu$ plane can be deformed into $C_n$. The Debye approximations in (3) are valid in this relevant region of the complex w-plane. Use of the conventional saddle point formula for evaluation of the integral in (5) then yields the geometrical ray series

$$G_o \sim e^{i\pi/4} \sqrt{\frac{2}{\pi k}} \sum_{n=0}^{\infty} (-1)^n \frac{e^{ikD_n}}{\sqrt{D_n}} \tag{8}$$

where

$$D_n = 2(n+1)\, a\sin\left(|\phi - \phi'| / 2(n+1)\right) \quad , \tag{8a}$$

each term of which corresponds to a direct or multiply reflected ray as depicted in Figure 2(a). The result in (8) could have been constructed directly by ray-optical techniques.

C. Mixed Ray-optical and Whispering Gallery Mode Representation

Although the series in (8) formally contains ray contributions with an arbitrarily large number of reflections, these are suspect since the saddle points, from which they are derived all cluster about $w = \pi/2$. Thus, the asymptotic method, whereby each saddle point is treated as isolated, is inadequate. Moreover, (3) becomes invalid as $w \to \pi/2$, thereby invalidating the simplification of the integrand, on which the saddle point evaluation is based. It is therefore necessary to truncate the number of legitimate ray-optical terms at some $n = N$ such that $w_{sN}$ is sufficiently less than $\pi/2$. With this in mind, one employs instead of (4) the partial expansion

$$\frac{1}{J'_\nu(ka)} = \frac{2}{H'^{(2)}_\nu(ka)} \sum_{n=0}^{N} (-1)^n r^n + \frac{1}{J'_\nu(ka)} (-1)^{N+1} r^{N+1} \tag{9}$$

When (9) is substituted into (1), one may write

$$G_o = G_{oN} + R_N \tag{10}$$

where $G_{oN}$ is given by (5) with the series truncated at $n = N$, and

$$R_N = -\frac{i}{\pi^2 ka} \int_{C'} \frac{e^{ika|\phi - \phi'|\sin w}}{H'^{(2)}_\nu(ka) J'_\nu(ka)} r^{N+1} (-1)^{N+1} \cos w\, dw \tag{11}$$

where $\nu = ka \sin w$. The asymptotic evaluation of $G_{oN}$ evidently yields ray contributions having experienced up to N reflections. The remainder integral $R_N$ incorporates the cumulative effects of ray fields having been reflected more than N times. It should be noted that when the observation point approaches the source point so that $|\phi - \phi'| \to 0$, one has $w_s \to \pi/2$ even for $n = 0$ and the ray representation fails altogether.

Several options are open for dealing with $R_N$. One possibility is to deform the integration path so as to minimize $|R_N|$. If C' is deformed into $C_N$ in Fig. 5, M residues at the poles $\nu_m$ of the integrand lying between C' and $C_N$ must be extracted. Thus, noting that $r = -1$ at $\nu_m$ (see (2) and (4)),

$$R_N = G_{oM} + R_{MN} \tag{12}$$

where

$$G_{oM} = \frac{i}{ka} \sum_{m=1}^{M} e^{i\nu_m|\phi - \phi'|} J_{\nu_m}(ka)\left[\frac{\partial}{\partial\nu} J'_\nu(ka)\right]^{-1}_{\nu_m} , \tag{13}$$

with $\nu_m = ka \sin w_m$ and $R_{MN}$ being the same as $R_N$ except for the replacement of C' by $C_N$. Each term in the series represents precisely one of the whispering gallery modes which make up the discrete spectrum in the previously mentioned Green's function representation in terms of angularly propagating waves. Since $w_m < \pi/2$, one may employ the Debye approximation in (3) to simplify (12). Thus, from (10) and (12),

$$G_o \sim G_{oN} + G_{oM} + R_{MN} . \tag{14}$$

D. Whispering Gallery Mode and Continuous Spectrum Representation

The spectral representation comprising the total discrete (whispering gallery mode) portion and a continuous portion may be obtained directly from (1).

As remarked in Section A, only those pole singularities having $\nu_m > 0$ yield spectral contributions in the angular transmission representation. When C in Fig. 4 is deformed into a contour extending along the imaginary $\nu$ axis, all necessary pole singularities are picked up and one is left with

$$G_o \sim G_{o\hat{M}} + \frac{1}{i(\pi ka)^2} \int_{-i\infty}^{+i\infty} \frac{e^{i\nu|\phi - \phi'|} d\nu}{H'^{(2)}_\nu(ka)\, J'_\nu(ka)} \tag{15a}$$

where $G_{o\hat{M}}$ is given by (13) and $\hat{M}$ is the total number of poles satisfying Re $\nu_m > 0$. The second member of (15a) is the continuous spectrum mentioned in Section A except that the spurious diffraction effects of the angular absorber are not present. By methods similar to Wasylkiwskyj (WASYLKIWSKYJ, W., 1975), this integral may be simplified considerably to

$$\frac{1}{\pi} \int_0^\infty e^{-ka|\phi - \phi'| \sinh v} dv , \quad ka >> 1 \tag{15b}$$

which is valid for $|\phi - \phi'|$ arbitrarily small. It is also pointed out that (15b) may be written as

$$\frac{1}{2}\left[\underline{H}_o(ka|\phi - \phi'|) - Y_o(ka|\phi - \phi'|)\right] \tag{15c}$$

where $\underline{H}_o$ is the Struve function and $Y_o$ the Neumann function which provides the correct singular behavior as $\phi \to \phi'$ .

E. Optimum Mix of Rays and Modes

The utility of the mixed ray - mode representation in (14) depends on the best choice of N and hence M so as to minimize $R_{MN}$ and render it negligible. Utilizing the asymptotic approximations in (3) to simplify the integrand of $R_{MN}$, Wasylkiwskyj (WASYLKIWSKYJ, W., 1975) has concluded that $R_{MN}$ can be neglected at observation points characterized by $w_{sM} \approx (w_M + w_{M+1})/2$, i.e., for saddle points well removed from the pole singularities. The justification is fairly loose and requires further study. It is likely that a precise choice is unimportant for very large ka and large separation of source and observation points. However, for moderate values of ka, or when the observer approaches the source, the problem must be addressed in a different manner.

Returning to the original expression for $G_o$ in (1), one may explore under what conditions the contributing range of the integrand is localized so that approximation methods may be used effectively. To this end, the cylinder functions are first replaced by their uniform asymptotic approximations in terms of Airy functions:

$$H'^{(2)}_\nu(ka) \sim -\sqrt{\frac{2\cos w}{\tau}} \frac{[Ai'(-\tau^2\Omega^{2/3}) + iBi'(-\tau^2\Omega^{2/3})]}{\Omega^{2/3}} , \quad \Omega = ka \tag{16}$$

$$J'_\nu(ka) \sim -\sqrt{\frac{2\cos w}{\tau}} \frac{Ai'(-\tau^2\Omega^{2/3})}{\Omega^{2/3}} \tag{17}$$

$$\tau = \frac{3}{2}\left(\cos w - \left(\frac{\pi}{2} - w\right)\sin w\right)^{1/3}, \quad \mathrm{Re}\, w > 0$$

When $\tau^2 (ka)^{2/3} >> 1$, these representations reduce to those in (3). Examining the behavior of the integrand over the contour C in the $\nu$-plane or the contour C' in the w-plane, Babich and Buldyrev have shown (BABICH, V. M. and BULDYREV, V. S., 1972) that the principal contribution to the integral arises from the vicinity of $\nu = ka$ or $w = \pi/2$ provided that the arc length parameter

$$\gamma = \left(\frac{ka}{2}\right)^{1/3} \frac{s}{a}, \quad s = a\left|\phi - \phi'\right|, \tag{18}$$

is bounded by the inequality*

$$\frac{2}{\sqrt{3}\,\Delta} \leq \gamma < 2\sqrt{\Delta}\left(\frac{ka}{2}\right)^{\delta}, \tag{19}$$

where $\Delta$ is a quantity of O(1) for moderate ka and $\delta$ is small and positive. Then changing variables to t via

$$\nu = ka + \left[\frac{ka}{2}\right]^{1/3} t \tag{20}$$

and using

$$H_\nu^{(2)\prime}(ka) \sim -\left(\frac{2}{ka}\right)^{2/3} w_2'(t)$$

$$J_\nu'(ka) \sim -\left(\frac{2}{ka}\right)^{2/3} Ai'(t) \tag{20a}$$

where

$$w_2(t) = Ai(t) + i\, Bi(t) \tag{20b}$$

one may write $G_o$ in the form

$$G_o \sim \frac{e^{iks}}{2i\pi\sqrt{ka}}\left(\frac{ka}{2}\right)^{2/3} \int_{\hat{C}} \frac{e^{i\gamma t}}{w_2'(t)\, Ai'(t)}\, dt \tag{21}$$

where the contour $\hat{C}$ in the t-plane is inferred from (20) and Fig. 4 by observing that $\nu = ka$ corresponds to $t = 0$ (note that the mappings $t_m$ and $t_p$ of $\nu_m$ and $\nu_p$, respectively, signify the zeros of Ai'(t) and $w_2'(t)$. Extracting ray optical contributions as in (10), when relevant, the form for $R_N$ analogous to (11) becomes

$$R_N = \frac{e^{iks}}{2i\pi\sqrt{ka}}\left(\frac{ka}{2}\right)^{2/3} \int_{\hat{C}} \frac{(-1)^{N+1}}{Ai'(t)\, w_2'(t)}\left[\frac{w_1'(t)}{w_2'(t)}\right]^{N+1} e^{i\gamma t}\, dt \tag{22}$$

Buldyrev and Lanin state as a criterion for the inclusion or not of the ray-optical series $G_{oN}$ the inequality

$$\frac{\gamma}{2\sqrt{\Delta}}\left(\frac{ka}{2}\right)^{-\delta} - 1 < (N+1) \leq \frac{\gamma}{2\sqrt{\Delta}}\left(\frac{ka}{2}\right)^{-\delta}, \tag{23}$$

with $\delta$ taken as (1/21). When the left-hand side of the inequality is negative, no ray-optical contributions are included. The canonical integral $R_N$ in (22) has been tabulated for N = -1, 0, 2 (BULDYREV, V. M. and LANIN, A. I., 1975).

* Ref. 2 actually deals with the Dirichlet problem $G_o = 0$ on the boundary. The validity of exactly the same condition for the Neumann function used here remains to be checked.

## F. Near Field and Infinite Plane Limits

The preceding results cannot account for the limiting case $\gamma \to 0$ in (18), which arises either when the observation point approaches the source point ($s \to 0$ with $a$ fixed) or when the radius of curvature becomes arbitrarily large ($a \to \infty$ with $s$ arbitrary but fixed). The latter limit traces the transition from a concave to a plane surface and, if $a$ is allowed to become negative, from concave to convex. We have derived the transition functions for these cases.

We begin with $G_o$ in (21) and use the Wronskian relation for the Airy functions together with Cauchy's theorem applied to the upper half of the $t$-plane to infer that, equivlently,

$$G_o \sim -\frac{e^{iks}}{2\pi ka}\left(\frac{ka}{2}\right)^{2/3} \int_{\hat{C}'} e^{i\gamma t}\,\frac{Ai(t)}{Ai'(t)}\,dt \tag{24}$$

with the contour $\hat{C}'$ passing below the real $t$ axis. Regarding the integral in (24) as a Laplace integral, the principal contribution for small $\gamma$ arises from the range of large $t$. Shifting the contour $\hat{C}'$ so that this is satisfied, and employing large argument expansions, one may show that

$$-\frac{Ai(t)}{Ai'(t)} \sim t^{-1/2}\left(1 - \frac{1}{4}t^{-3/2} + \frac{7}{32}t^{-3\cdots}\right), \quad -\pi < \arg t < 0 \tag{25}$$

Then by Laplace inversion of (24),

$$G_o \sim \frac{i}{2} H_o^{(1)}(ks)\left\{1 + \frac{e^{-i\pi/4}}{4}\sqrt{\pi}\,\gamma^{3/2} - \frac{i7\gamma^3}{60} + O(\gamma^{9/2})\right\} \tag{26}$$

Actually, the inversion yields for the factor outside the braces the large argument approximation of $(i/2)\,H_o^{(1)}(ks)$ the Green's function for an infinite perfectly conducting plane. By inserting the exact limiting value for $a \to \infty$, the formula in (26) may be applied as well in the near field of the source.

To trace the transition from concave to convex curvature when the distance $s$ along the surface remains fixed, we allow $a$ to change continuously from positive to negative values via the complex excursion $0 \le \arg a \le \pi$. To keep $a = a|\phi - \phi'|$ positive, it is necessary simultaneously to have $\arg|\phi - \phi'| = -\arg a$. Moreover, one must continuously deform the integration path in the complex $t$-plane to keep the integral convergent ($\exp(i\gamma t)$ oscillatory) when $\gamma$ is allowed to become complex according to the rules stated above. These conderations lead to a straight line path along which $\arg t = -\pi/3,\ 2\pi/3$, when $\arg a = \pi$. Changing variables $t = \mu \exp(i2\pi/3)$, one finds

$$G_o \sim -\frac{e^{iks}}{2\pi ka}\left(\frac{ka}{2}\right)^{2/3} \int_{C_\mu} \frac{w_1(\mu)}{w_1'(\mu)}\,e^{i\gamma\mu}\,d\mu \tag{27}$$

where $\gamma$ is again given by (18) and the path $C_\mu$ proceeds along the real $\mu$ axis. The expression in (27) is the known result for the field on the surface of a convex perfectly conducting cylinder. By contour deformation about the singularities $\mu_p$ at $w_1'(\mu_p) = 0$, one derives the creeping wave series, and by expansion analogous to (25) and Laplace inversion the limiting transition as $\gamma \to 0$ (HASSERJIAN, G. and ISHIMARU, A., 1972). Thus, one may track the field continuously as the curvature changes from concave to convex between fixed source and observation points on the surface.

## G. Generalization to Variable Curvature

Invoking the principle of locality, which characterizes high frequency propagation and diffraction, one may generalize the preceding results to accommodate concave surfaces with slowly variable radius of curvature $a(s)$. The results are as follows. For the integral representation in (21):

$$G_o \sim -\frac{e^{iks}}{4\pi[f(0)f(s)]^{1/2}} \int_{\hat{C}'} e^{ikDt}\,\frac{Ai(t)}{Ai'(t)}\,dt \quad , \tag{28}$$

where the source point is located at $s = 0$, $s$ is the distance between the source and observation points measured along the surface, and

$$f(s) = \left(\frac{ka(s)}{2}\right)^{1/3}, \qquad D(s) = \frac{1}{2}\int_0^s \frac{d\mu}{f^2(\mu)} \tag{29}$$

$R_N$ in (22) is treated in the same manner (BABICH, V.M. and BULDYREV, V.S., 1972). As $D(s) \to 0$, with s small, one may derive the generalization of (26),

$$G_o \sim \frac{i}{2} H_o^{(1)}(ks)\left\{1 + \frac{e^{-i\pi/4}}{4}\sqrt{\pi}\,(kD)^{3/2} + O(kD)^3\right\} \tag{30}$$

The ray-optical series $G_{oN}$ in (10), with (8), becomes (BABICH, V.M. and BULDYREV, V.S., 1972)

$$G_o \sim e^{i\pi/4}\sqrt{\frac{2}{\pi k}} \sum_{n=0}^{\infty} (-i)^n \frac{e^{ikD_n}}{\sqrt{D_n}} D_n \tag{31}$$

where $D_n$ is the divergence coefficient incorporating the effects of surface curvature.

$$D_1 = \sqrt{\frac{a_1(\ell_1+\ell_2)\cos\theta}{2\ell_1\ell_2 - a(\ell_1+\ell_2)\cos\theta_1}}$$

$$D_2 = \sqrt{a_1 a_2 \cos\theta_1 \cos\theta_2 (\ell_1+\ell_2+\ell_3)} \tag{31a}$$

$$\sqrt{} = \sqrt{4\ell_1\ell_2\ell_3 + a_1 a_2(\ell_1+\ell_2)\cos\theta_1\cos\theta_2 - 2\ell_1\ell_2 a_2\cos\theta_2}$$

$$- 2\ell_3 a_1(\ell_1+\ell_2)\cos\theta_1 - 2\ell_1\ell_3 a_2\cos\theta_2 + a_1 a_2 \ell_3 \cos\theta_1\cos\theta_2 \tag{31b}$$

with $a_i$ the surface radius of curvature and $\theta_i$ the ray angle with respect to surface normal of the i-th reflection. Finally, the asymptotically approximated (see (3)) whispering gallery mode series $G_{oM}$ in (13),

$$G_{oM} \sim -\frac{i}{2} \frac{e^{iks}}{[f(0)f(s)]^{1/2}} \sum^{M} \frac{e^{ikDt_m}}{t_m} \tag{32}$$

It should be noted that (28) cannot be used when a(s) changes continuously from positive to negative values unless the source is located near the inflection point $a = \infty$, where (30) and its convex counterpart applies. The failure of (28) for arbitrary source location on the concave portion arises from the fact that the function $f(s) \to \infty$ as s nears the inflection point. On the other hand, D remains finite. The coefficient nullifies the finite integral.

### H. Numerical Results

Some numerical calculations in the literature illustrate the utility of the various representations for the Green's function $G_o$. Wasylkiwskyj (WASYLKIWSKYJ, W., 1975) has evaluated the field on a concave circular perfectly conducting surface by summing the whispering gallery mode series and the continuous spectrum contribution in (15) (Figure 6). Although he employed this method of computation, the interpretation of the result, as stated by him, is in fact achieved via the ray-optical formulation since the oscillations in the curve are due to interference between the direct ray and reflected rays. Wasylkiwskyj observes that the mixed representation in (14), while useful for interpretation, offers no numerical advantage. It appears nevertheless that this aspect would warrant further study. When ka is changed the corresponding curve for $|G_o|$ may be obtained from that in Fig. 6 by a scaling law (WASYLKIWSKYJ, W., 1975), thus making a typical curve universal for other cases.

When ka and (or) $\gamma$ is relatively small, it is appropriate to explore the representation in (10). This was done by Buldyrev and Lanin (BULDYREV, V.M. and LANIN, A.I., 1975) for a concave surface of parabolic shape, for which the asymptotic results could be checked against the exact series solution. The calculation utilized tabulated values for $G_o$ in (28) or $R_N$ in (22) (when generalized as in (28) to variable curvature), and the ray series in (31), with N determined from (23) ($\gamma$ there is replaced by kD). One observes from the typical curve in Fig. 7 that the asymptotic representation in (28), when modified to account for the different boundary condition on $G_o$, does not adequately predict the field for kD so large that a ray-optical term can be separated out. As kD increases further, each formula with a lower N value than permitted is less accurate than that with the correct N value. This demonstration shows indeed the important role played by the geometrical optics field.

## III. CONCAVE BOUNDARY WITH SURFACE IMPEDANCE CONDITION

To address the problem of ground wave propagation, we assume that the ground characteristics can be taken into account by a constant surface impedance Z. For the circular cylinder, this implies the

boundary condition

$$\frac{\partial G}{\partial \rho} = ikZ'G \quad \text{at } \rho = a \quad , \quad Z' = \frac{Z}{\zeta} \tag{33}$$

where $\zeta$ is the impedance of free space. By proceeding as in Section II, one may show that the following modified expressions apply:

Instead of (1),

$$G_o = \frac{1}{i(\pi ka)^2} \int \frac{e^{i\nu|\phi|}\, d\nu}{\left[H_\nu'^{(2)}(ka) - iZ'H_\nu^{(2)}(ka)\right]\left[J_\nu'(ka) - iZ'J_\nu(ka)\right]} \tag{34}$$

Instead of (4), the traveling wave expansion involves

$$\frac{1}{J_\nu'(ka) - iZ'J_\nu(ka)} = \frac{2}{H_\nu'^{(2)}(ka) - iZ'H_\nu^{(2)}(ka)} \sum_{n=0}^{\infty} (-1)^n r^n \quad , \quad |r| < 1 \tag{35}$$

$$r = \frac{H_\nu'^{(1)}(ka) - iZ'H_\nu^{(1)}(ka)}{H_\nu'^{(2)}(ka) - iZ'H_\nu^{(2)}(ka)} \tag{35a}$$

with corresponding modification of (5). The saddle points in (7) are unchanged, and the ray-optical series (8) becomes

$$G_o \sim e^{i\pi/4}\sqrt{\frac{2}{\pi k}} \sum_{n=0}^{\infty} (-i)^n \frac{(\Gamma_n)^n \cos^2 w_n}{(\cos w_n + Z')^2} \frac{e^{ikD_n}}{\sqrt{D_n}} \tag{36}$$

where $\Gamma_n$ is the boundary reflection coefficient for ray species n,

$$\Gamma_n = \frac{\cos w_n - Z'}{\cos w_n + Z'} \tag{37}$$

and

$$\cos w_n = \sin \frac{|\phi - \phi'|}{2(N+1)} \quad , \quad D_n = 2a(n+1)\sin \frac{|\phi - \phi'|}{2(n+1)} \tag{38}$$

The whispering gallery mode series is

$$G_{oM} = \frac{i}{ka} \sum_{m=1}^{M} e^{i\nu_m|\phi - \phi'|} J_{\nu_m}(ka) \left[\frac{\partial}{\partial \nu}\left[J_\nu'(ka) - iZ'J_\nu(ka)\right]\right]^{-1}_{\nu_m} \tag{39}$$

where the summation extends over the zeros $\nu_m$ defined by

$$J_{\nu_m}'(ka) - iZ'J_{\nu_m}(ka) = 0 \tag{40}$$

The remainder term (11) becomes

$$R_N = \frac{i}{\pi^2 ka} \int_C \frac{e^{ika|\phi - \phi'|\sin w}\,(r^{N+1})(-1)^{N+1}\cos w\, dw}{\left[H_\nu'^{(2)}(ka) - iZ'H_\nu^{(2)}(ka)\right]\left[J_\nu'(ka) - iZ'J_\nu(ka)\right]} \tag{41}$$

where r is given by (35a). The analogue of (21) becomes

$$G_o \sim \frac{e^{iks}}{2i\pi^2(ka)} \left(\frac{ka}{2}\right)^{2/3} \int_{\hat{C}} \frac{e^{i\gamma t}}{[w_2'(t) + i\alpha w_2(t)]\,[Ai'(t) + i\alpha Ai(t)]}\, dt \tag{42}$$

where $\alpha = Z' \left(\frac{ka}{2}\right)^{1/3}$. Under the same conditions, one has for $R_N$ in (22),

$$R_N \sim \frac{e^{iks}}{2i\pi^2(ka)} \left(\frac{ka}{2}\right)^{2/3} \int_{\hat{C}} \frac{(-1)^{N+2}}{w_2'(t) + i\alpha w_2(t)} \frac{r^{N+1}\, e^{i\gamma t}}{Ai'(t) + i\alpha Ai(t)}\, dt \tag{43}$$

Employing the Wronskian, the field may be put in the form of (24)

$$G_o \sim -\frac{e^{iks}}{2\pi ka} \left(\frac{ka}{2}\right)^{2/3} \int_{\hat{C}} \frac{e^{i\gamma t}\, Ai(t)}{Ai'(t) + i\alpha Ai(t)}\, dt \tag{44}$$

The perturbation expansion

$$-\frac{Ai(t)}{Ai'(t) + i\alpha Ai(t)} \sim \frac{1}{\sqrt{t}} \left[1 + \frac{i\alpha}{\sqrt{t}} - \frac{\alpha^2}{t} - \left(\frac{1}{4} + i\alpha^3\right) \frac{1}{t^{3/2}} + O(t^{-2})\right] \tag{45}$$

leads from (44) to the representation

$$G_o \sim \frac{e^{iks + i\frac{\pi}{4}}}{\sqrt{2\pi ks}} \left[1 - e^{-i\pi/4} \sqrt{\pi}\, \gamma^{1/2}\, \alpha - 2i\alpha^2\gamma + \left(\frac{1}{4} + i\alpha^3\right) \sqrt{\pi}\, \gamma^{3/2}\, e^{-i\pi/4} + O(\gamma^2)\right] \tag{46}$$

thereby generalizing (26).

## REFERENCES


1. BABICH, V. M. and BULDYREV, V. S., 1972, Asymptotic Methods of Short Wave Diffraction, Moscow, USSR: Nauka, Chapter 11, Section 4.

2. BULDYREV, V. M. and LANIN, A. I., Jan. 1975, "Asymptotic Formulas for a Wave Propagating Along a Concave Surface; Limits of Their Applicability," Radio Tekh. Elektron. Vol. 20.

3. FELSEN, L. B., and MARCUVITZ, N., 1973, Radiation and Scattering of Waves, Englewood Cliffs, NJ: Prentice Hall, Inc., Sections 3.3, 3.4.

4. HASSERJIAN, G. and ISHIMARU, A., May-June 1962, "Currents Induced on the Surface of a Conducting Circular Cylinder by a Slot," J. Res. Nat. Bur. Stand., Vol. 66D, No. 3, pp. 335-365.

5. KINBER, B. YE., 1961, "On the Diffraction of Electromagnetic Waves by a Concave Surface of a Circular Cylinder," Radio Tekh.Elektron; Vol. 6, No. 8, pp. 1273-1283.

6. WASYLKIWSKYJ, W., July 1975, "Exact and Quasi-Optic Diffraction within a Concave Cylinder," IEEE Transactions on Antennas and Propagation, Vol. AP-23, No. 4, pp. 480-492.

FIG. 1 General surface contour

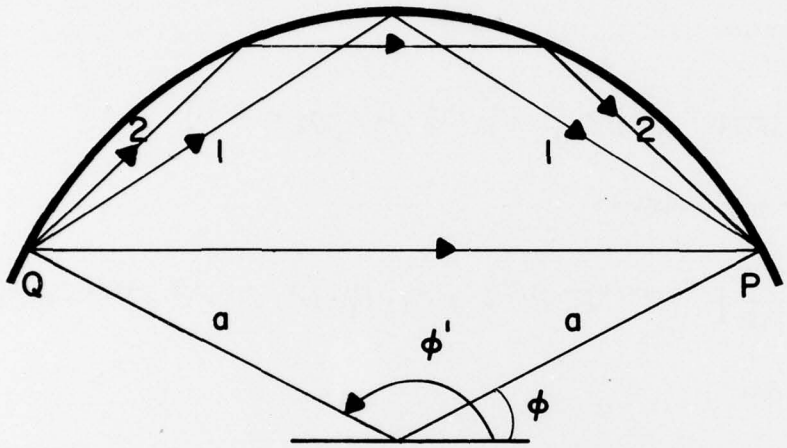


a) direct and multiply reflected rays

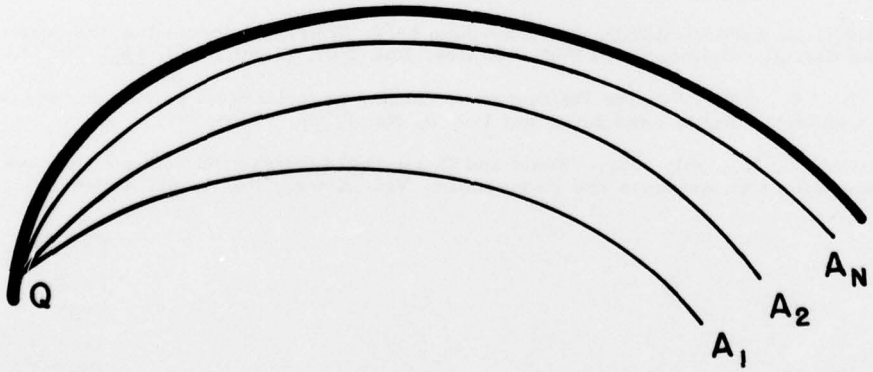


b) caustics $A_n$ for rays reflected N times; these ray contributions are confined to the region between $A_n$ and the boundary

FIG. 2 Rays and caustics for a circular boundary

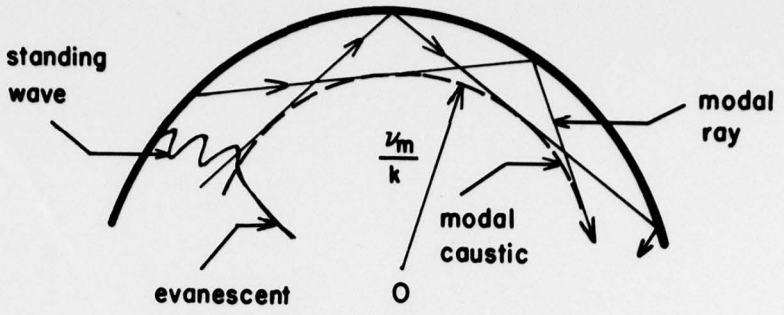


FIG. 3 Whispering gallery mode: modal field, modal rays and caustic ($\nu_m = ka \sin w_m$)

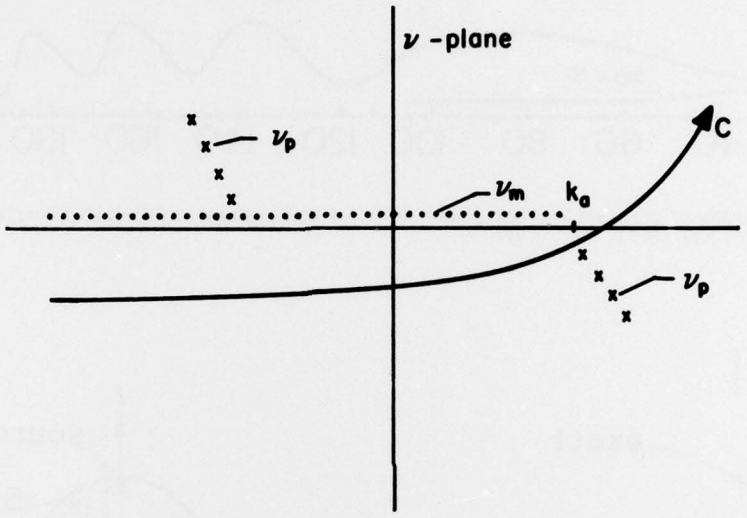


FIG. 4 Integration path and singularities in complex $\nu$ -plane
x -- zeros $\nu_p$ of $H_\nu^{(2)}(ka)$; . -- zeros $\nu_m$ of $J_\nu'(ka)$

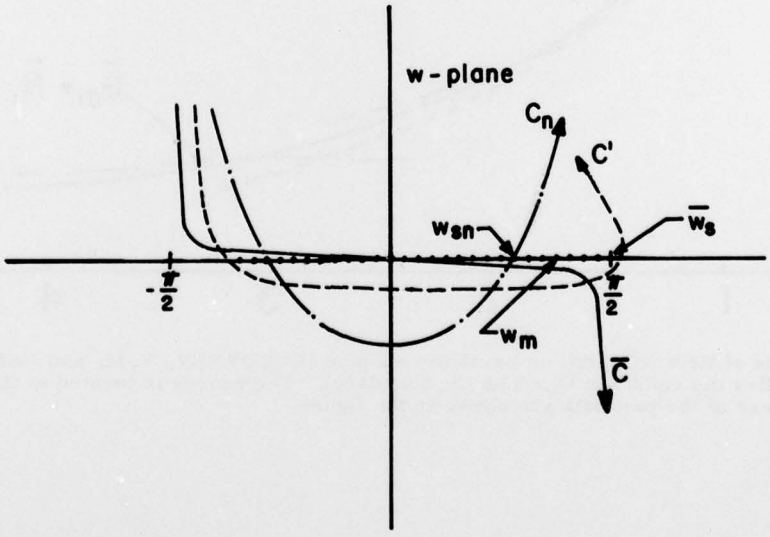


FIG. 5 Integration paths and singularities in complex w plane ($\nu = ka \sin w$). $\bar{C}$ corresponds to C in Fig. 4 and can be changed to C' because of symmetries in the integrand in (5). C' in turn can be deformed into the steepest descent path $C_n$ through $w_{sn}$. The pole singularities $w_m$ arising from the zeros of $J_\nu'(ka)$ do not affect the asymptotic evaluation of (5). The poles $w_p$ are not shown.

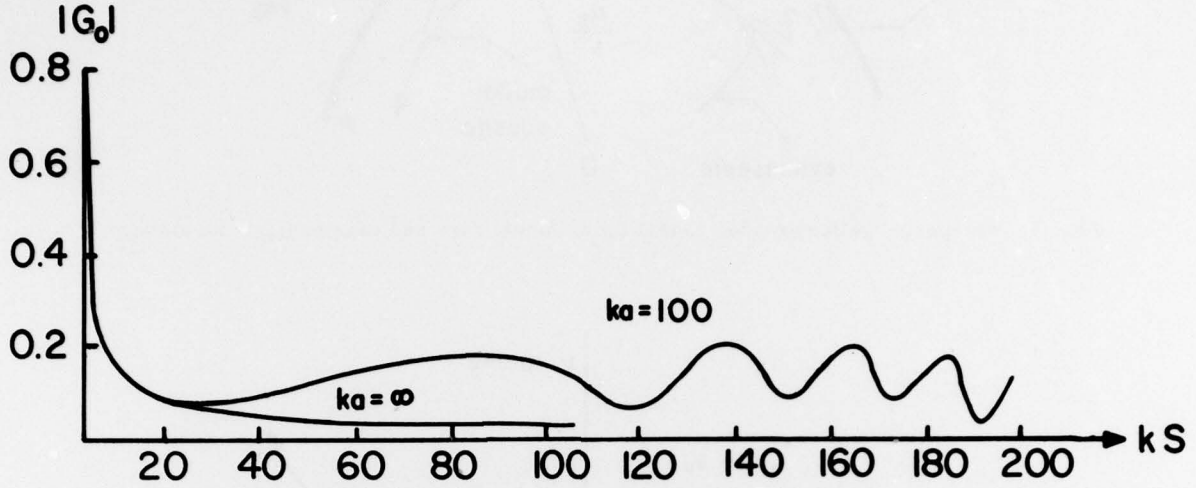


FIG. 6 Magnitude of field on infinite plane (ka = ∞) and concave cylindrical surface (ka = 100) (WASYLKIWSKYJ, W., 1975)

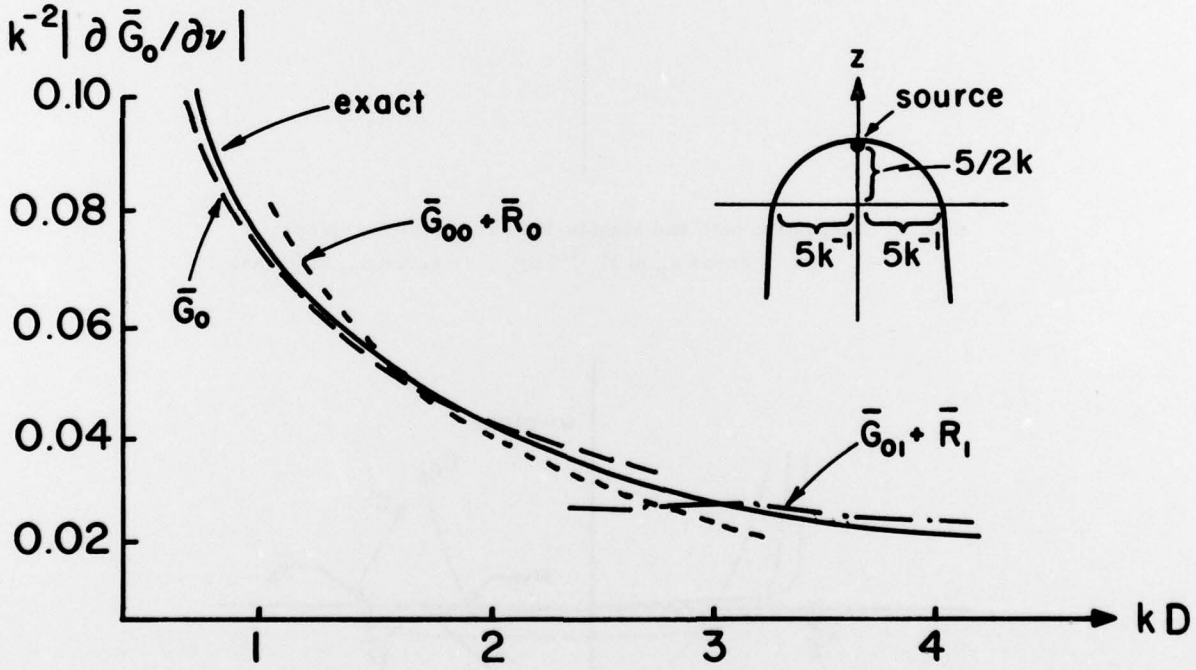


FIG. 7 Magnitude of field ($\partial \bar{G}_0/\partial \nu$) on parabolic surface (BULDYREV, V. M. and LANIN, A. I., 1975); $\bar{G}_0$ satisfies the condition $\bar{G}_0 = 0$ on the boundary). The source is located at the apex, and the parameters of the parabola are shown in the figure.

## DISCUSSION

K.D.Becker: In 1951, B.Friedman showed that, in the case of an ideally conducting sphere, the continuous spectrum is vanishing. Is there in your case a connection with the sign of curvature of an ideally conducting surface and the existence of a continuous spectrum?

L.B.Felsen: The existence or not of a continuous spectrum depends on the choice of the representative theorem. In the problem which I discussed in cylindrical geometry, the field was represented in terms of angularly propagating waves in an infinity-extended angular space. Therefore, the spectral-theorem has to be developed for the radial domain. For the interior of the cylinder, with the origin (cylinder axis) accessible, one finds both, a discrete and a continuous spectrum. When the origin is shielded by another cylindrical boundary, the spectrum is purely discrete.